This is a repository copy of *Direct Photonic Coupling of a Semiconductor Quantum Dot and a Trapped Ion*.

White Rose Research Online URL for this paper:
http://eprints.whiterose.ac.uk/97374/

Version: Supplemental Material

Article:

Meyer, H.M., Stockill, R., Steiner, M. et al. (7 more authors) (2015) Direct Photonic Coupling of a Semiconductor Quantum Dot and a Trapped Ion. Physical Review Letters (PRL), 114 (12). ARTN 123001. ISSN 0031-9007

https://doi.org/10.1103/PhysRevLett.114.123001

Reuse

Items deposited in White Rose Research Online are protected by copyright, with all rights reserved unless indicated otherwise. They may be downloaded and/or printed for private study, or other acts as permitted by national copyright laws. The publisher or other rights holders may allow further reproduction and re-use of the full text version. This is indicated by the licence information on the White Rose Research Online record for the item.

Takedown

If you consider content in White Rose Research Online to be in breach of UK law, please notify us by emailing eprints@whiterose.ac.uk including the URL of the record and the reason for the withdrawal request.

eprints@whiterose.ac.uk
https://eprints.whiterose.ac.uk/

Supplemental Material : Direct photonic coupling of a semiconductor quantum dot and a trapped ion

H. M. Meyer,[1,2] R. Stockill,[1] M. Steiner,[1,*] C. Le Gall,[1] C. Matthiesen,[1]
E. Clarke,[3] A. Ludwig,[4] J. Reichel,[5] M. Atatüre,[1,†] and M. Köhl[1,2,‡]

[1] *Cavendish Laboratory, University of Cambridge,*
JJ Thomson Avenue, Cambridge CB3 0HE, United Kingdom
[2] *Physikalisches Institut, University of Bonn, Wegelerstrasse 8, 53115 Bonn, Germany*
[3] *EPSRC National Centre for III-V Technologies,*
University of Sheffield, Sheffield, S1 3JD, UK
[4] *Lehrstuhl für Angewandte Festkörperphysik,*
Ruhr-Universität, 44780 Bochum, Germany
[5] *Laboratoire Kastler Brossel, École Normale Supérieure, 24 Rue Lhomond, 75005 Paris, France*

This PDF file includes:

- QD optical characterization
- Determination of the absorption probability per photon p_{abs}
- Modelling of the photonic link
- Photon Transfer Efficiency
- Preparation of the QD electron spin mixture

QD OPTICAL CHARACTERIZATION

We present the measured optical properties of the neutral QD which was used in Fig. 1-3 of the main manuscript. Fig. 1(a) is an intensity correlation measurement of the QD resonance fluorescence which demonstrates the single-photon nature of the QD emission. From this measurement and from the lifetime measurement presented in Fig. 1(b), we can infer an excited-state lifetime $T_1 = 640$ ps, corresponding to a decay rate, Γ, of $2\pi \times 250$ MHz. We verify through Fabry-Perot scans the portion of coherent scattering from the QD, as shown in the spectra of Fig. 1(c) and 1(d). We also extract spectral wandering, and pure dephasing from modeling these spectra (described in section 4), resulting in the solid curves in Fig. 1(c) and 1(d).

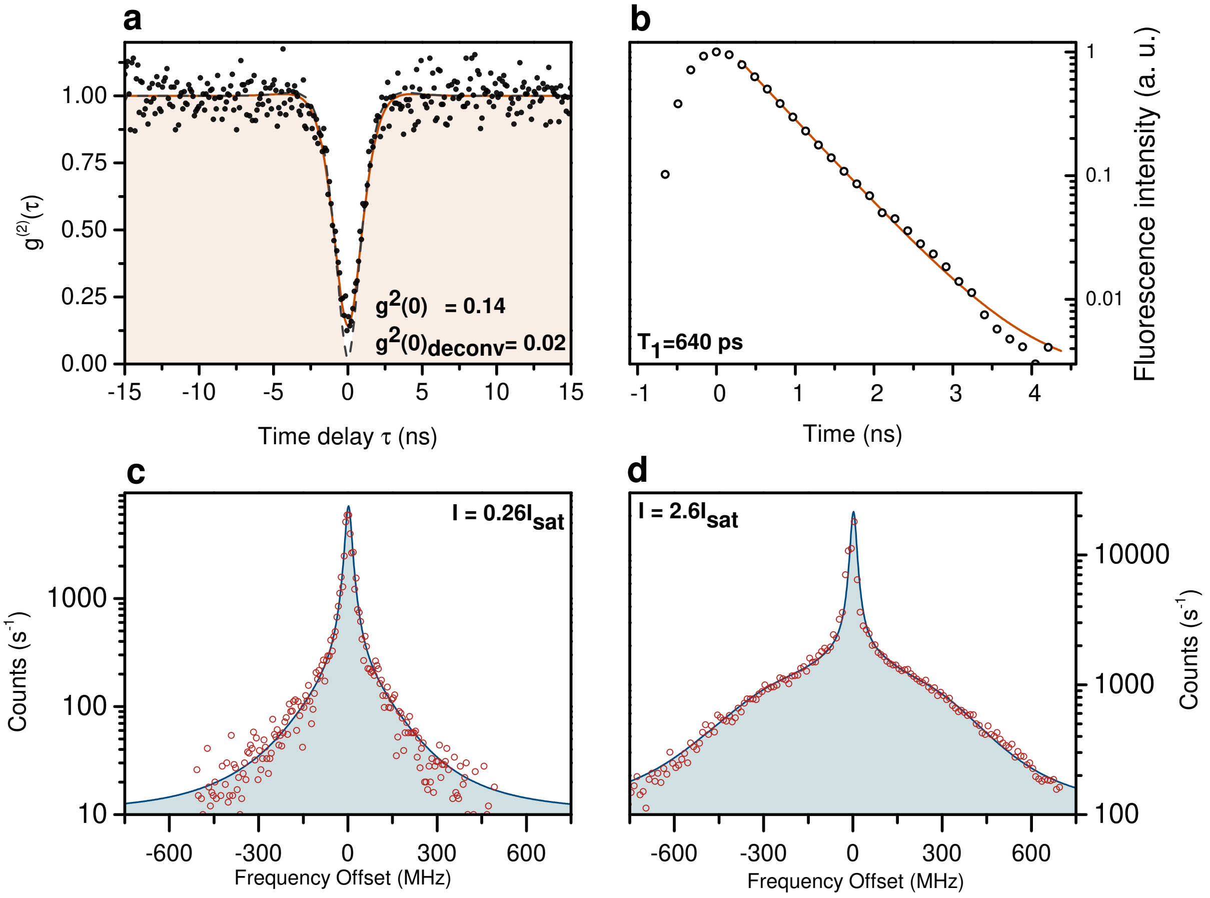

Figure S 1. **QD characterization.** (a) Intensity correlation of the QD resonance fluorescence. The solid curve is a fit to the data, including spectral wandering of the transition and the response time of the detectors. The dashed curve is the autocorrelation that would be expected with an infinitely fast response. (b) Time-resolved fluorescence of the QD under pulsed excitation, showing a decay of 640 ps. (c) & (d) Emission spectra of the QD for different excitation intensities, recorded with a scanning Fabry-Perot cavity. The solid lines are theoretically expected spectra, convolved with the 30 MHz width of the cavity. The theory includes pure dephasing, as detailed in section 4, and spectral wandering of the QD resonance of 300 MHz. The spectra are recorded at zero magnetic field, resulting in spectral fluctuations differing from those measured in the main experiment.

DETERMINATION OF THE ABSORPTION PROBABILITY PER PHOTON p_{abs}

The experimental sequence used to determine the absorption probability per photon p_{abs} consists of four phases [cf. Fig. 2].

- **Initialization** The ion is prepared in the $m_J = -3/2$ Zeeman level of the ${}^2\text{D}_{3/2}$ state by applying σ^- and π polarized 935 nm light in combination with 369 nm light. The 935 nm beam has an angle of 75 degrees with respect to the cavity axis and the 369nm beam is transverse to it. After 120 μs, approximately 90% of the population is accumulated in the target state.
- **Probe** For a time $T_{\text{interact}} = 0 - 1500\,\mu$s the QD fluorescence is guided onto the fiber-cavity. The cavity length is actively stabilized to be resonant with the ${}^3\text{D}[3/2]_{1/2}$-${}^2\text{D}_{3/2}$ transition of ${}^{174}\text{Yb}^+$ for all experiments presented in the main text. During T_{interact} we record the number of photons reflected from the cavity. From this measurement we determine the average number of QD-photons $\bar{n}$ which impinged upon the cavity by taking account of the finite cavity in-coupling, attenuation on the optical path, background light and dark-counts of the photon detectors. The corresponding QD-photon rate is then $\gamma_{\text{QD}} = \bar{n}/T_{\text{interact}}$.
- **Readout** In order to prove that the ion has been interacting with a QD photon during T_{interact} we make use of the large branching ratio from the ${}^3\text{D}[3/2]_{1/2}$ to the ${}^2\text{S}_{1/2}$ state. Since the ${}^3\text{D}[3/2]_{1/2}$ state decays mainly to the ${}^2\text{S}_{1/2}$ state we define p_{abs} as the probability per photon to transfer population from ${}^2\text{D}_{3/2}$ to ${}^2\text{S}_{1/2}$. The effect of the QD photons is then determined by subsequent scattering of 369 nm light on the ${}^2\text{P}_{1/2}$-${}^2\text{S}_{1/2}$ transition of the ion.

  Fig. 2(b) shows the 369 nm fluorescence detected by a photo-multiplier tube (PMT) during the read-out phase. The fluorescence signal decays exponentially if the ion is in ${}^2\text{S}_{1/2}$ state (black curve). This decay occurs because the 369 nm transition is not cyclic. In contrast, for an ion in the ${}^2\text{D}_{3/2}$ state the read out signal is constant; the finite signal amplitude arises from background light (blue curve). The red curve shows the signal for a stream of QD photons. The ${}^2\text{D}_{3/2}$ to ${}^2\text{S}_{1/2}$ transfer probability p_{transfer} for the QD probe pulse is calculated by integrating the PMT counts during the first 19 μs of the readout phase for the three traces, giving $c_{\text{D-state}}$,$c_{\text{S-state}}$ and c_{QD}:

  $$p_{\text{transfer}} := \frac{c_{\text{QD}} - c_{\text{D-state}}}{c_{\text{S-state}} - c_{\text{D-state}}}\,. \tag{1}$$

  p_{abs} is determined from p_{transfer} and the mean number of photons $\bar{n}$:

  $$p_{\text{abs}} := \frac{\Gamma_{\text{abs}}}{\gamma_{\text{QD}}} = \frac{-\ln(1-p_{\text{transfer}})}{T_{\text{interact}}}\frac{T_{\text{interact}}}{\bar{n}} = \frac{-\ln(1-p_{\text{transfer}})}{\bar{n}}\,. \tag{2}$$

  As not every excitation to ${}^3\text{D}[3/2]_{1/2}$ state leads to decay to the ${}^2\text{S}_{1/2}$ state p_{abs} underestimates the actual excitation probability. From the cavity-QED parameter we infer that the altered branching ratio is 91% in favour of the decay to ${}^2\text{S}_{1/2}$ state and therefore our measurements systematically underrate p_{abs} by 9%.
- **Doppler cooling** Finally, the ion is continuously laser-cooled on the ${}^2\text{P}_{1/2}$-${}^2\text{S}_{1/2}$ transition for 160 μs.

MODELING OF THE PHOTONIC LINK

The spectrum of the QD emission $S(\nu)$ is given by the Fourier transform of the two-time correlation function of the optical dipole $\langle\sigma_+(\tau)\sigma_-(0)\rangle$. To calculate the QD spectrum, we consider a two-level

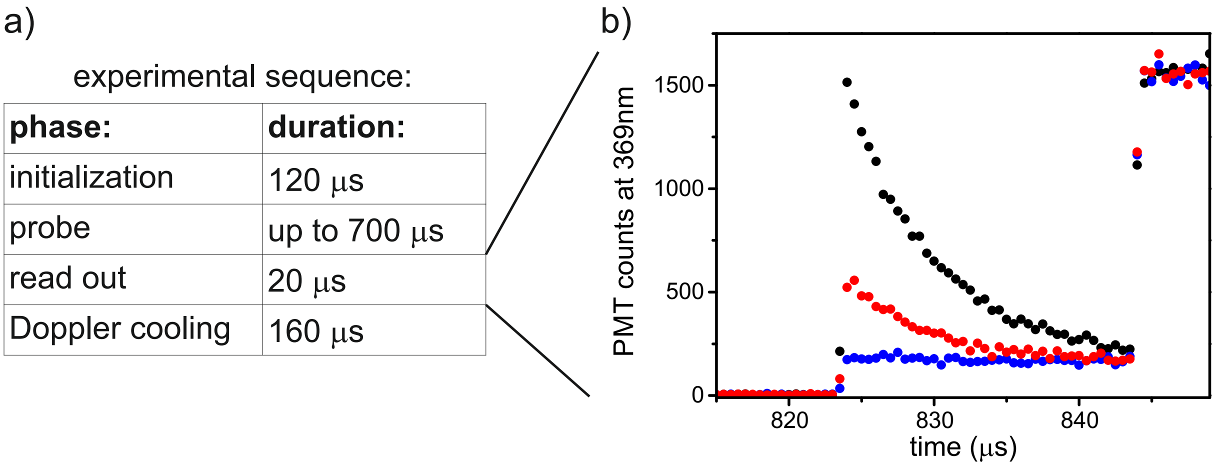

experimental sequence:

phase:	duration:
initialization	120 µs
probe	up to 700 µs
read out	20 µs
Doppler cooling	160 µs

Figure S 2. **^{174}Yb^{+} initialization and readout.** (a) Experimental sequence. (b) Time-resolved 369 nm fluorescence of the ion during the read out phase (starts at $t = 824\,\mu$s). Black curve: ion is in the bright ^{2}S$_{1/2}$ state. Blue curve: ion is in the dark ^{2}D$_{3/2}$ state. Red curve: the QD-photons transferred the ion partially from the dark to bright state. Each curve represents the accumulated data from 50000 repetitions.

system interacting with a classical field in the rotating wave approximation (e.g. [1]) with an additional pure dephasing term γ of the optical dipole. The relevant physical quantities are:

- The excited state decay rate $\Gamma = 2\pi \times 250$ MHz.
- The QD-laser Rabi coupling Ω, or equivalently, the normalized intensity $I/I_{sat} \propto \Omega^2/\Gamma^2$.
- An intensity-dependent dephasing rate of the optical dipole $\gamma = 2\pi \times (I/I_{sat}) \times 9.3$ MHz.
- The frequency of the laser ν_L.
- The detuning between the laser and the optical dipole frequency $\delta = \nu_{QD} - \nu_L$.
- The frequency of the ion ν_0.

The number of QD photons $n_{QD\to Ion}(\nu_0)$ spectrally overlapping with the ion resonance is:

$$n_{QD\to Ion}(\nu_0) = \int S(\nu)L(\nu_0 - \nu)d\nu\,, \tag{3}$$

where $L(\nu_0 - \nu)$ is a Lorentzian of FWHM of 20 MHz corresponding to the width of the cavity-mediated ion absorption.

The transfer rate from ^{2}D$_{3/2}$ to ^{2}S$_{1/2}$ (Γ_{abs}) is assumed to be proportional to $n_{QD\to Ion}(\nu_0)$, with a correction for a small portion of laser photons n_L which leak to the ion due to finite polarization rejection:

$$\Gamma_{abs} \propto n_{QD\to Ion}(\nu_0) + n_L * L(\nu_0 - \nu_L)\,. \tag{4}$$

And the absorption probability per photon is proportional to:

$$p_{abs}^{model} \propto \frac{n_{QD\to Ion}(\nu_0) + n_L * L(\nu_0 - \nu_L)}{n_{QD} + n_L}\,, \tag{5}$$

where n_{QD} is the total number of QD photons. The modeled p_{abs}^{model} is scaled to fit the observation. The scaling factor is governed by the ion-cavity coupling.

The QD signal to laser leakage is 70 : 1 at saturation. Consequently, in the modeling, we take:

$$n_L(I_{sat}) = n_{QD}(I_{sat})/70 \tag{6}$$
$$n_L(I) \propto I\,. \tag{7}$$

In order to model the spectrum, shown in Fig. 3(a) of the text, we computed p_{abs}^{model}, as a function of $\nu_0 - \nu_L$. Having measured the lifetime of the QD, the QD dipole dephasing rate and the FWHM of the ion absorption through the cavity independently, the detuning is the only free parameter. The asymmetry observed experimentally in Fig. 3(a), main text, results from the combined effect of optically induced dephasing and detuning [2]. The theoretical curve in Fig. 3(a) of the main text illustrates such an imbalance with $\delta = 250\,\text{MHz}$ and $\gamma = 2\pi \times 93\,\text{MHz}$. Detuning is set by a non-linear feedback mechanism known as dragging: the QD transition is locked to the resonant laser, and the locking point is determined by hyperfine interaction between the optically created electron and the nuclei in the QD [3–5]. Typical absorption scans, taken for two different scanning speeds and excitation intensities, are presented in Fig. 3. As shown in the figure, higher excitation intensities and slower scanning speeds permit a build up of nuclear polarization, holding the QD resonance to the excitation frequency. The emission profile is exactly the same as in the absence of dragging. This dragging of the QD transition is used for tuning the emission spectrum presented in Fig. 3(a) of the main manuscript.

p_{abs}^{model} is computed for $\nu_0 = \nu_{QD} = \nu_L$ as a function of the normalized excitation intensity I/I_{sat} to model the intensity-dependent absorption shown in Fig. 3(b) of the main text. The modeled evolution is scaled to fit the data. This scaling factor is governed by the ion-cavity coupling. An excitation-dependent pure dephasing term has been included, for consistency with the spectrum modelling in Fig. 3(a) of the main text, but its effect is below our experimental resolution.

For semiconductor QDs, relaxation between the dressed states induced by acoustic phonons sets a lower bound to the dephasing rate observed at a given Rabi frequency [2, 6]. For a saturation parameter $I/I_{sat} = 10$, a dephasing rate on the order of $0.1 - 1\,\text{MHz}$ is to be expected from such processes. For this QD, a much larger intensity dependent dephasing rate was measured which is likely to be caused by fast electrical field noise in this sample. Excitation intensity-dependent spectral wandering (i.e. slow electrical field fluctuations) with a 160 MHz amplitude at $I/I_{sat} = 1$ and a 250 MHz amplitude at $I/I_{sat} = 5$ as well as on-off switching of the fluorescence were also observed. The effect of spectral wandering in the modeling was found to be a small correction compared to the accuracy of the data points, so it was not included in our final analysis.

In the main manuscript, we estimate a 20% increase of the efficiency of a coherent scheme over a incoherent scheme for a direct state-transfer protocol. Here are the details of the assumptions which go into this estimate. Our results show that, within error bars, coherently scattered photons are absorbed as efficiently as CW laser photons ($\eta_{ion} \propto \int \delta(\nu) L_{Ion}(\nu)$) and more generally, ($\eta_{ion} \propto \int S_{QD}(\nu) L_{Ion}(\nu)$) where $L_{Ion}(\nu)$ is the ion absorption linewidth (20MHz) and $S_{QD}(\nu)$ is the QD emission linewidth. If coherently scattered photons are to be used, spin has to be mapped onto a photon which is then sent to the ion. Because of the probabilistic nature of coherent scattering, if p is the probability of scattering one photon, p^2 is the probability of scattering two photons. Two-photon scattering events are a source of error (the quantum state of the spin can be mapped on one and only one photon). Hence, the coherent scattering probability has to be $p \ll 1$. We took $p_{coh} = 0.1$. On the other hand, for an incoherently scattered QD photon, the best state-transfer you can hope for is if you take $p_{incoh} = 1$, and $S_{QD}(\nu)$ is a Lorentzian with a 250MHz linewidth (that is assuming a lifetime limited QD-photon coherence, which is a best case scenario). The 20% improvement refers to the overall efficiency $p \times \eta_{ion}$ for the coherent versus incoherent case.

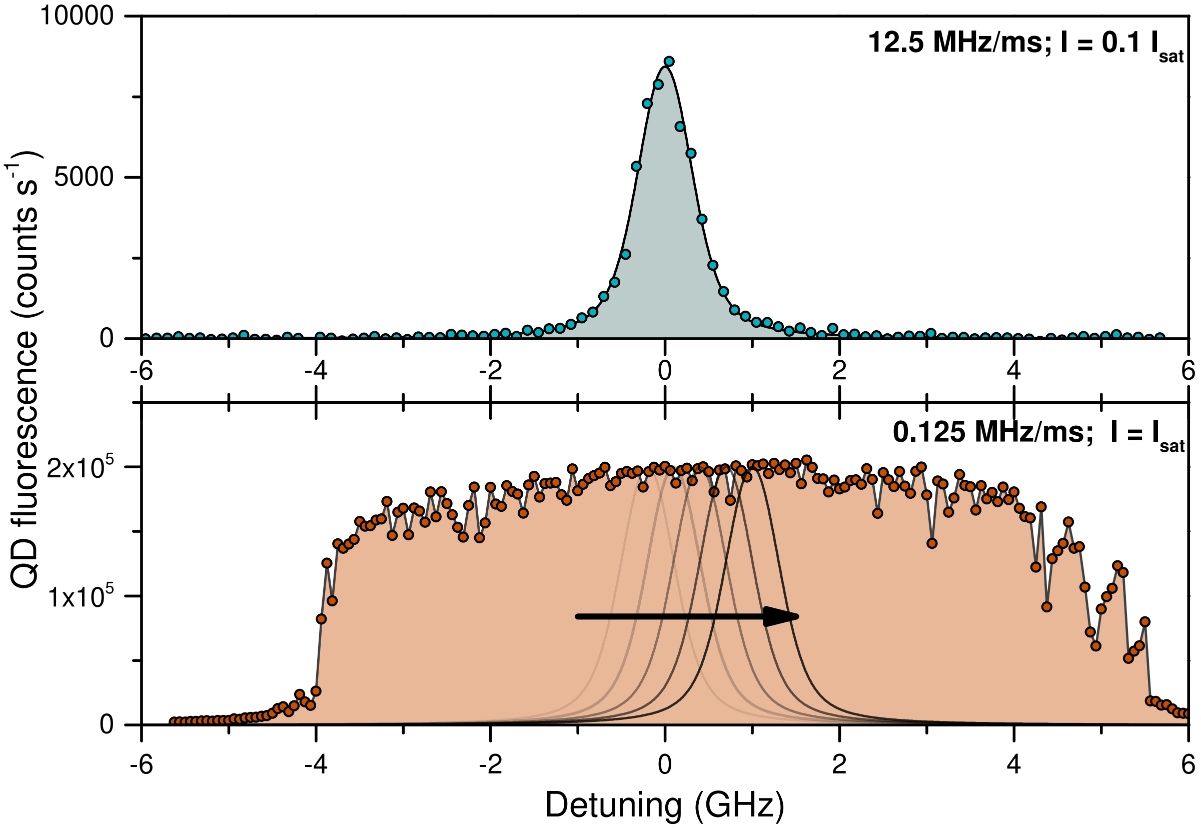

Figure S 3. **QD absorption scans.** Absorption scans of the neutral QD used in the main manuscript. If the laser scanning rate is sufficiently slow, strong deviation from a Lorentzian lineshape can be observed as a hyperfine field develops to ensure through an effective Zeeman shift that the QD transition remains nearly resonant with the laser frequency. The Lorentzian curves shown in the bottom panel illustrate how the absorption profile is continuously shifted to follow the laser.

PHOTON TRANSFER EFFICIENCY

In addition to the ion state transfer per photon probabilities reported there is a constant transfer efficiency from the QD to the ion cavity of 5×10^{-4}, as mentioned in the main text. This can be partitioned into two main stages: photon out-coupling from the QD sample (3.5%) and losses in the path from the sample to the ion cavity (1.4% transmission). A large proportion of the losses between the QD sample and the ion cavity can be attributed to the need to monitor photon rates between the systems, as well as polarization control between the QD and the ion.

The quoted transmission can be recovered from the individual elements which make up the link from the QD sample to the ion cavity: QD microscope beam splitters (90% × 2 transmission), linear polarizer (41%), coupling into the QD microscope fiber (40%), coupling into the 50-m fiber (70%), polarization optics transmission at 50-m fiber output (90%), polarization filtering (50%), beam splitter transmission (90% × 2) and coupling into the fiber cavity (42%).

PREPARATION OF THE QD ELECTRON SPIN MIXTURE

In order to demonstrate a dependence of the ion absorption on the spin state of a QD, we split the transitions of a negatively charged QD with an external magnetic field applied along the growth axis ($B = 0.7\,\mathrm{T}$). While polarization-spin correlations are erased by our cross-polarization technique, energy-spin correspondence is used to provide a spin-selective absorption.

The energy of the transitions is found by mapping the intensity of the resonance fluorescence as a function of laser frequency and gate voltage as shown in Fig. 4(a). Strong fluorescence is observed when the gate voltage is set to 0.4 V (0.55 V) corresponding to fast co-tunneling as the electron occupation changes from 0 to 1 (1 to 2) in the QD. Fast co-tunneling randomizes the spin-state of the electron, preventing spin shelving following optical pumping. Between these two co-tunneling regions, a strong reduction of fluorescence occurs due to optical pumping. The fluorescence can be recovered using a second repump laser as shown in Fig. 4(b) [7].

To fully characterize the optical pumping, we perform a time-resolved pulsed two-color experiment [Fig. 4(c)]. Two pulses are generated from cw laser sources using acousto-optic modulators. A 3 μs pulse at 320552 GHz resonantly drives the red transition at a power corresponding to $I/I_{sat} = 2$. The emission rate of red photons decreases exponentially in time as the electron is pumped into the $|\uparrow\rangle$ state. Then, a 6.5 μs pulse at 320571 GHz resonantly drives the blue transition at $I/I_{sat} = 0.5$. Again, the emission rate decreases exponentially as a consequence of optical pumping, this time into the $|\downarrow\rangle$ state. From these, we can estimate a preparation fidelity of 92.2% $\pm\, 0.2\%$ (92.8% $\pm\, 0.2\%$) in the state $|\uparrow\rangle$ ($|\downarrow\rangle$).

In the experiment showing spin-selective absorption of the ion, we use pulses which only differ from the previous experiment by their duration: the pulse resonant with the red transition has a variable duration between 0 and 700 ns, which is used to create an incoherent spin superposition $p_\uparrow |\uparrow\rangle\langle\uparrow| + p_\downarrow |\downarrow\rangle\langle\downarrow|$ with $p_\uparrow$ varying between 0.072(2) and 0.81(1). Photons are then generated, mostly coherently, by a 550 ns pulse resonant with the blue transition. Time-resolved resonance fluorescence traces corresponding to identical experimental conditions are presented in Fig. 4(d). In this protocol, the 935 nm generation pulse is kept constant, so that the change of ion absorption can only be attributed to a change of spin preparation of the QD electron.

---

[*] present address:Centre for Quantum Technologies, National University of Singapore, 3 Science Drive 2; Singapore 117543, Singapore

[†] Electronic address: ma424@cam.ac.uk

[‡] Electronic address: michael.koehl@uni-bonn.de

[1] M. O. Scully and M. S. Zubairy, *Quantum Optics* (Cambridge University Press, 1997).

[2] A. Ulhaq, S. Weiler, C. Roy, S. M. Ulrich, M. Jetter, S. Hughes, and P. Michler, Optics Express **21**, 4382 (2013).

[3] C. Latta, A. Hogele, Y. Zhao, A. N. Vamivakas, P. Maletinsky, M. Kroner, J. Dreiser, I. Carusotto, A. Badolato, D. Schuh, W. Wegscheider, M. Atature, and A. Imamoglu, Nat Phys **5**, 758 (2009).

[4] I. T. Vink, K. C. Nowack, F. H. L. Koppens, J. Danon, Y. V. Nazarov, and L. M. K. Vandersypen, Nature Physics , 764 (2009).

[5] A. Högele, M. Kroner, C. Latta, M. Claassen, I. Carusotto, C. Bulutay, and A. Imamoglu, Phys. Rev. Lett. **108**, 197403 (2012).

[6] A. J. Ramsay, A. V. Gopal, E. M. Gauger, A. Nazir, B. W. Lovett, A. M. Fox, and M. S. Skolnick, Phys. Rev. Lett. **104**, 017402 (2010).

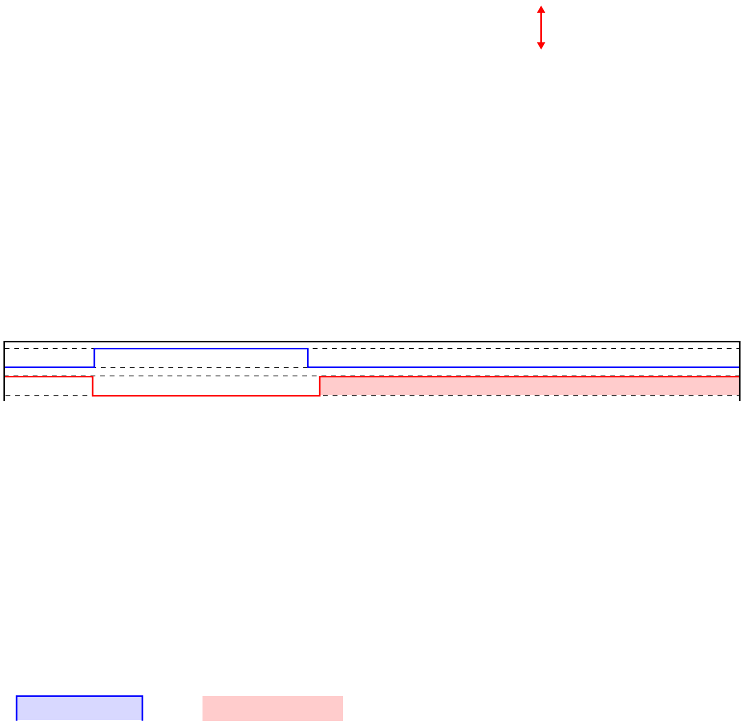[7] M. Atatüre, J. Dreiser, A. Badolato, A. Hgele, K. Karrai, and A. Imamoglu, Science **312**, 551 (2006).